Received: 29 May 2022 | Accepted: 4 July 2022

DOI: 10.1002/prp2.992

INVITED REVIEW

Tetramisole is a new I_{K1} channel agonist and exerts I_{K1}-dependent cardioprotective effects in rats

Qinghua Liu[1] | Jiaxing Sun[1] | Yangdou Dong[1] | Pan Li[1] | Jin Wang[2,3] | Yulan Wang[2,3] | Yanwu Xu[4] | Xinrui Tian[5] | Bowei Wu[2,3] | Peifeng He[6] | Qi Yu[6] | Xuechun Lu[7] | Jimin Cao[2,3]

[1]Department of Pathophysiology, Shanxi Medical University, Taiyuan, China

[2]Key Laboratory of Cellular Physiology, Ministry of Education, Shanxi Medical University, Taiyuan, China

[3]Department of Physiology, Shanxi Medical University, Taiyuan, China

[4]Department of Biochemistry, Shanghai University of Traditional Chinese Medicine, Shanghai, China

[5]Department of Respiratory and Critical Care Medicine, Second Hospital of Shanxi Medical University, Taiyuan, China

[6]Shanxi Key Laboratory of Big Data for Clinical Decision Research, School of Management, Shanxi Medical University, Taiyuan, China

[7]Department of Hematology, The Second Medical Center, Chinese PLA General Hospital, National clinical research center for geriatric disease, Beijing, China

Correspondence
Qi Yu, Xuechun Lu and Jimin Cao, Key Laboratory of Cellular Physiology at Shanxi Medical University, Ministry of Education, and Department of Physiology, Shanxi Medical University. 56 Xinjian South Road, Taiyuan 030001, China, Emails: yuqi@sxmu.edu.cn, luxuechun@126.com, caojimin@sxmu.edu.cn

Funding information
Key Laboratory of Medical Electrophysiology (Southwest Medical University), Ministry of Education of China, Grant/Award Number: KeyME-2017-04; Key R&D Program of Shanxi Province, Grant/Award Number: 201903D311011; National Natural Science Foundation of China, Grant/Award Number: 82170523; National Social Science Fund of China, Grant/Award Number: 21BTQ050; Natural Science Foundation of Shanxi Province, Grant/Award Number: 20210302123309; Open Fund from Key Laboratory of Cellular

Abstract

Cardiac ischemia, hypoxia, arrhythmias, and heart failure share the common electrophysiological changes featured by the elevation of intracellular Ca^{2+} (Ca^{2+} overload) and inhibition of the inward rectifier potassium (I_{K1}) channel. I_{K1} channel agonists have been considered a new type of anti-arrhythmia and cardioprotective agents. We predicted using a drug repurposing strategy that tetramisole (Tet), a known anthelmintic agent, was a new I_{K1} channel agonist. The present study aimed to experimentally identify the above prediction and further demonstrate that Tet has cardioprotective effects. Results of the whole-cell patch clamp technique showed that Tet at 1–100 μmol/L enhanced I_{K1} current, hyperpolarized resting potential (RP), and shortened action potential duration (APD) in isolated rat cardiomyocytes, while without effects on other ion channels or transporters. In adult Sprague–Dawley (SD) rats in vivo, Tet showed anti-arrhythmia and anticardiac remodeling effects, respectively, in the coronary ligation-induced myocardial infarction model and isoproterenol (Iso, i.p., 3 mg/kg/day, 10 days) infusion-induced cardiac remodeling model. Tet also showed anticardiomyocyte remodeling effect in Iso (1 μmol/L) infused adult rat ventricular myocytes or cultured H9c2 (2-1) cardiomyocytes. Tet at 0.54 mg/kg in vivo or 30 μmol/L in vitro

Abbreviations: AP, action potential; APD, action potential duration; ARVM, adult rat ventricular myocyte; AS, Andersen syndrome; CaMKII, calmodulin-dependent protein kinase II; ChIP, channel interacting proteins; DAD, delayed afterdepolarization; EF, ejection fraction; FS, fractional shortening; HBSS, Hank's Balanced Salt Solution; HE, hematoxylin and eosin; HF, heart failure; HPF, high-powered field; I_{K1}, inward rectifier potassium channel; Iso, isoproterenol; LV, left ventricle; MAGUK, membrane-associated guanylate kinase; MI, myocardial infarction; p-PKA, phosphorylated protein kinase A; PVC, premature ventricular contraction; RP, resting potential; SD, Sprague–Dawley; Tet, tetramisole; VF, ventricular fibrillation; VT, ventricular tachycardia.

Physiology (Shanxi Medical University), Ministry of Education, China, Grant/Award Number: KLMEC/SXMU-201909

showed promising protections on acute ischemic arrhythmias, myocardial hypertrophy, and fibrosis. Molecular docking was performed and identified the selective binding of Tet with Kir2.1. The cardioprotection of Tet was associated with the facilitation of I_{K1} channel forward trafficking, deactivation of PKA signaling, and inhibition of intracellular calcium overload. Enhancing I_{K1} may play dual roles in anti-arrhythmia and antiventricular remodeling mediated by restoration of Ca^{2+} homeostasis.

KEYWORDS
arrhythmia, calcium overload, cardiac remodeling, drug repurposing, inward rectifier potassium channel, molecular docking, tetramisole

1 | INTRODUCTION

Cardiac ischemia, hypoxia, malignant arrhythmias, and heart failure (HF) are the leading causes of morbidity and mortality in cardiovascular diseases.[1,2] Convincing data have shown that these cardiac diseases share the common electrophysiological changes in ventricles, such as prolongation of the action potential duration (APD), elevation of intracellular Ca^{2+} (Ca^{2+}-overload), and decrease of inward rectifier potassium channel (I_{K1}).[3,4] Ventricular I_{K1} channels, primarily constituted by Kir2.1 channel subunit (encoded by KCNJ2 gene), play key roles in maintaining the resting potential (RP), establishing the excitation threshold, and contributing to the final repolarization of the action potential (AP).[5,6] Inhibition of I_{K1} might elicit electrical disturbance, including RP depolarization, APD prolongation, and Ca^{2+} overload, ultimately initiating triggered arrhythmias. Further, Ca^{2+} overload activates Ca^{2+}-activated signaling associated with cardiac remodeling.[7,8] Theoretically, I_{K1} should be a promising anti-arrhythmic and antiremodeling target. Enhancing/upregulation of I_{K1} is compensation for I_{K1} deficit and a novel modulation for cardiac Ca^{2+} homeostasis. Flecainide, a widely used I anti-arrhythmic drug, exhibits effective control over ventricular arrhythmias in Andersen syndrome (AS) associated with loss of function mutations in KCNJ2.[9,10] Caballero et al unraveled that flecainide increases Kir2.1/I_{K1} channels, an effect underlies the pharmacological rescue of AS-associated ventricular arrhythmias.[11] However, due to the multifaceted influence of flecainide on ionic channels, the mechanisms of flecainide therapy may be comprehensive and complex. We reported a selective I_{K1}/Kir2.1 channel agonist, zacopride, and showed its striking anti-arrhythmic effect in anesthetic rats postacute myocardial infarction (MI) or in conscious rats with healing MI.[3,12] Zacopride also attenuated maladaptive cardiac repair following MI, Iso-, or L-thyroxine- toxicosis.[13–15] So far, zacopride is the only documented selective I_{K1} channel agonist. Developing more pharmacological tools is an issue to support the theoretical link between I_{K1} agonism and cardioprotection.

Drug repurposing (also known as drug repositioning, drug reprofiling) is to rediscover new uses for existing drugs. Compared with traditional de novo drug development, it has been an alternative method in the advantage of reducing the costs and time-to-market of a medication.[16–18] This strategy is largely driven by integrating, analyzing, and interpreting the data generated by high-throughput DNA and RNA sequencing, mass spectrometry, metabolomics and transcriptomic data, phenotyping, clinical data, etc. These data are often referred to as big data.[16] In the present study, we took a drug repurposing strategy and found that tetramisole (Tet) might be a potential I_{K1} agonist, anti-arrhythmic, and antiventricular remodeling drug.

Tet is an anthelminthic agent used in veterinary applications to treat helminth or worm infections. It is a racemic mixture of (+) and (−) isomers. The (−) isomer (levamisole) accounts for most of the biological activity of tetramisole.[19] The whole-cell patch clamp technique was applied to identify whether Tet is a selective I_{K1} agonist by comparing its potential influences on other channels or transporters, such as voltage-gated Na^+ channel (I_{Na}), L-type Ca^+ channel (LTCC, $I_{Ca\text{-}L}$), transient outward K^+ channel (I_{to}), sustained outward K^+ current (I_{Ksus}), and Na^+-Ca^{2+} exchanger (I_{NCX}). We further observed the effects of Tet on RP, AP, and intracellular calcium. Acute MI-induced arrhythmias and Iso-induced ventricular remodeling model were established to clarify whether increasing I_{K1} is a feasible anti-arrhythmic and antiremodeling strategy.

2 | MATERIALS AND METHODS

2.1 | Animal and ethical approval

Male Sprague–Dawley (SD) rats (2 months old) were provided by the Laboratory Animal Research Center of Shanxi Medical University (Taiyuan, China). The rats were housed under standard conditions, room temperature 20–24°C, humidity 40%–60%, 12:12 h light-dark cycles with light intensity up to 200 lux, and fed standard chow and water ad libitum. This study was carried out in accordance with the recommendations of the guidelines for the Care and Use of Laboratory Animals (NIH, revised 2011), and approved by the Ethics Committee of Shanxi Medical University (No. SYDL2021004).

2.2 | Isolation of adult rat ventricular myocytes

Single adult rat ventricular myocytes (ARVMs) were isolated using an enzymatic dissociation procedure. In brief, a rat heart was

quickly removed and mounted via the aorta on an 80 cm H_2O high Langendorff retrograde perfusion apparatus. The heart was perfused first with oxygenated Ca^{2+}-free Tyrode's solution (at 37°C) for approximately 10 min, then with collagenase P (0.1 g/L; Roche)-Tyrode solution for about 20 min. The composition of the Tyrode's solution was (in mmol/L): NaCl 135, KCl 5.4, $CaCl_2$ 1.8, $MgCl_2$ 1.0, NaH_2PO_4 0.33, HEPES 10, glucose 10, pH adjusted to 7.3–7.4 with NaOH. When the heart was well digested, the left ventricle (LV) was separated, minced, and filtrated in KB solution with the composition (in mmol/L): KOH 85, L-glutamic acid 50, KCl 30, $MgCl_2$ 1.0, KH_2PO_4 30, glucose 10, taurine 20, HEPES 10, EGTA 0.5, pH adjusted to 7.4 with KOH. The isolated myocytes were stored at room temperature (23–25°C) at least 2 h before use.

2.3 | Patch clamp

Isolated ARVMs suspension was transferred to a chamber mounted on an inverted microscope (Nikon Diaphot; Nikon Co.) and superfused with Tyrode's solution. The whole-cell recording was performed with an amplifier Axopatch 200B (Molecular Device) or Patchmaster EPC10 (HEKA Electronic). Filled with the pipette solution, the electrode resistance was maintained at 2–5 MΩ except for 1–1.5 MΩ for Na^+ current recording. The current signal was filtered at 2 kHz and sampled at 10–20 kHz. Current recordings were performed in the voltage clamp mode, and APs were recorded in the current clamp mode at a frequency of 1.0 Hz. Currents or APs were recorded in the presence of tetramisole (Sigma) at different concentrations (1, 10, 30, and 100 μmol/L) compared with baseline recording. The currents were expressed in terms of cell capacitance (pA/pF). All experiments were conducted at room temperature (23–25°C) except 36°C for APs recordings.

To measure AP, Tyrode's solution was used as the extracellular solution. The pipette solution contained (in mmol/L) KCl 150.0, $MgCl_2$ 1.0, EGTA 5.0, HEPES 5.0, K_2-ATP 3.0, and the pH adjusted to 7.3 with KOH. The membrane potentials were corrected for the liquid junction potential (8 mV).

For I_{K1} recording, Tyrode's solution was applied as the extracellular solution except for 0.2 mM $CdCl_2$ used to block $I_{Ca\text{-}L}$. The pipette solution contained (in mmol/L): KCl 150.0, $MgCl_2$ 1.0, EGTA 5.0, HEPES 5.0, K_2-ATP 3.0, and 4-aminopyridine (4-AP) 5.0, pH 7.4 adjusted with KOH. $BaCl_2$ (0.2 mmol/L) was used to block I_{K1} channels. I_{K1} was determined as Ba^{2+}-sensitive current.

For I_{Na} recording, the extracellular solution contained (in mmol/L) NaCl 60.0, CsCl 5.0, $CdCl_2$ 0.1, $MgCl_2$ 2.5, glucose 10.0, 4-AP 5.0, HEPES 5.0, saccharose 80.0, and pH 7.4 achieved with NaOH. The pipette solution contained (in mM) EGTA 11.0, KCl 130.0, Na_2-ATP 5.0, HEPES 10.0, $MgCl_2$ 2.0, $CaCl_2$ 1.0, 4-AP 5.0, and pH 7.2 adjusted with CsOH.

For $I_{Ca\text{-}L}$ measurement, Tyrode's solution was used as the extracellular solution. The pipette solution contained (in mM) EGTA 5.0, KCl 150.0, K_2-ATP 3.0, HEPES 5.0, 4-AP 5.0, $MgCl_2$ 1.0, Mg-ATP 1.0, and pH 7.3 adjusted with KOH.

The extracellular solution for I_{to} and I_{Ksus} recordings was Tyrode's solution adding 0.1 mmol/L$CdCl_2$ and 0.2 mmol/$BaCl_2$ used to block $I_{Ca\text{-}L}$ and I_{K1}, respectively. The pipette solution contained (in mM) KCl 150.0, $MgCl_2$ 1.0, EGTA 5.0, HEPES 5.0, K_2-ATP 3.0, and pH 7.3 adjusted with KOH.

To measure I_{NCX}, the extracellular solution contained (in mmol/L) NaCl 140.0, $CaCl_2$ 2.0, $MgCl_2$ 2.0, glucose 10.0, HEPES 5.0, and pH 7.4 adjusted with CsOH. In addition, the Na^+-K^+ pump, K^+ channel, and Ca^{2+} channel were blocked by 0.02 mmol/L ouabain, 1.0 mmol/L $BaCl_2$, 2.0 mmol/L CsCl, and 1.0 μmol/L nicardipine, respectively. The pipette solution contained (in mM) EGTA 42.0, $CaCl_2$ 29.0, $MgCl_2$ 13.0, potassium aspartate 42.0, K_2-ATP 10.0, Na_2-creatinephosphate 5.0, 4-AP 20.0, HEPES 5.0, and pH 7.4 with CsOH. I_{NCX} could be blocked by a high concentration of Ni^{2+} at 5.0 mmol/L.

2.4 | Induction of ischemic arrhythmias and preexposure with tetramisole

Arrhythmias were induced by ligating the left main coronary artery as previously described (Huang et al., 2001).[20] After anesthetized with sodium pentobarbital (65 mg/kg, i.p.), rats were ventilated at 60 strokes/min and a stroke volume of 30 ml/kg by a small animal respirator (DH-1; Chengdu Instrument Factory) to maintain normal blood pO_2, pCO_2, and pH. The right femoral vein was cannulated for drug administration. Body temperature was maintained with an air conditioner. A left thoracotomy was performed in the fourth intercostal space. After opening the pericardium, a 6–0 suture was placed around the proximal portion of the left coronary artery, and the artery was ligated for 15 min. Myocardial ischemia was certified by elevation of the ST segment. Pharmacological treatments were as follows: Tet 0.18, 0.54, 1.8 mg/kg, Tet + chloroquine (CQ, I_{K1} antagonist, 7.5 μg/kg). The agent was dissolved in 0.2 ml of saline and administered intravenously 3 min before coronary artery occlusion. The control rat received 0.2 ml saline.

Prior to ischemia, a Lead II electrocardiogram (ECG) was continuously recorded with a waveform data analysis software (RM6240, BiopacSystem, Chengdu Instrument Factory). The rats exhibiting spontaneous arrhythmias were discarded. The ventricular ectopic activity was evaluated according to the diagnostic criteria advocated by Lambeth Convention.[21] The ECGs were analyzed to determine the individual episode of arrhythmias, total episodes, and episode duration of ventricular tachyarrhythmias, including premature ventricular contraction (PVC), ventricular tachycardia (VT), and ventricular fibrillation (VF).

2.5 | Pretreatment with tetramisole and detection of Kir2.1 expression

Rats were randomly divided into MI, Tet pretreatment (0.54 mg/kg/day), and Tet + CQ (7.5 μg/kg/day) groups. The agents or saline was

administrated by intraperitoneal injection once a day for 10 days. Then acute ischemic arrhythmia was established by ligating the left anterior descending artery. ECGs were recorded to observe the effects of Tet pretreatment on arrhythmias. The effect of Tet on Kir2.1 expression was observed by Western blotting.

2.6 | Induction of cardiac hypertrophy and remodeling

Cardiac hypertrophy was induced by daily injection of Iso (3 mg/kg/day; Sigma) for 10 days in rats in vivo. Pharmacological treatments were as follows: Iso, Tet (0.54 mg/kg/day, i.p.), Iso + Tet, and Iso + Tet + CQ (7.5 μg/kg/day, i.p.). Control rats were administered with the same volume of saline. The dose of Tet and CQ were applied according to our previous study[13] and preliminary experiment. Ventricular remodeling was evaluated by echocardiography and histology.

2.7 | Echocardiography

The GE Vivid 7 Pro Ultrasound System (10 S probe, probe frequency 8.0 MHz, equipped with 2D strain imaging software, and EchoPAC workstation) was used in M-mode for rodent hearts. Approximate exploration angle was at 15–30°, depth at 2–3 cm, frame rate > 250/s, and maximum frame rate up to 400/s. The positioning criterion was the LV long-axis section. The measured parameters included LV dimensions at end-diastole (LVIDd) and end-systole (LVIDs), interventricular septum thickness at end-diastole (IVSd) and end-systole (IVSs), LV posterior wall thickness at end-diastole (LVPWd) and end-systole (LVPWs), and LV ejection fraction (EF) and LV short-axis fractional shortening (FS).

2.8 | Histology

Samples of LV from all groups were fixed in 10% phosphate buffered formalin and subjected to routine histological processing. Transverse LV sections (5 μm thick) were cut using a cryostat microtome (Leica). After hematoxylin and eosin (HE) staining, the cross-sectional area of myofibers was measured using a microscope (Olympus) under a high-powered field (HPF) (×400 magnification). Fibrosis was evaluated by Masson's trichrome staining, and the collagen content in the interstitial space was estimated by analyzing the images of each group. Total collagen area was calculated and expressed as the percent of the total ventricular area under HPF.

2.9 | Induction of cardiomyocyte remodeling

In vitro remodeling models were established by Iso infusion in native ARVMs or H9c2 (2-1) cells (National Collection of Authenticated Cell Cultures).

Adult rat ventricular myocytes were isolated and subjected to gradient recalcification using a modified Tyrode's solution (containing 0.5% BSA and 1.2 mM $CaCl_2$). Then the cells were randomly subdivided into four groups, control, Iso (1 μmol/L), Iso + Tet (30 μmol/L), Iso + Tet + $BaCl_2$ (1 μmol/L), and treated with agents for 24 h. In parallel, ARVMs postwell recalcification were randomly subdivided into four groups, control, Iso (1 μmol/L), Iso + Tet (30 μmol/L), Iso + Tet + $BaCl_2$ (1 μmol/L), and a 1-h pharmacological treatment was performed before calcium imaging.

H9c2 (2-1) cardiomyocytes were derived from rat hearts and exhibit many of the properties of cardiac muscle, including calcium transporters and associated machinery,[22] and Kir2.1 expression.[23] In the in vitro study, we applied $BaCl_2$ as an I_{K1} blocker to clarify the underlying relationship between cardioprotection and I_{K1} regulation. The cells were randomly divided into 10 groups: normal control, Tet 1, 10, 30, 100 μmol/L, Iso infusion (1 μmol/L), Iso + Tet (10 μmol/L), Iso + Tet (30 μmol/L), Iso + Tet10 + $BaCl_2$ (1 μmol/L), Iso + Tet30 + $BaCl_2$. After 48-h incubation, cells were collected for Western blotting. Besides, cells were seeded in a 24-well plate or 35 mm plates and treated with the above-mentioned agents for 48 h. The resting $[Ca^{2+}]_i$ of cardiomyocytes was detected by laser confocal microscopy.

2.10 | $[Ca^{2+}]_i$ Imaging

The intracellular Ca^{2+} fluorescence in native ARVMs was indicated by the dual-wavelength Ca^{2+} indicator Fura-2 AM (Dojindo Laboratories). Post-24 h of pharmacological treatment, the cells were incubated with 3 μM Fura-2 AM in the dark at 37°C for 30 min then washed three times with Tyrode's solution.

The intracellular Ca^{2+} fluorescence in cultured H9c2 (2-1) cells was indicated either by single-wavelength Ca^{2+} indicator Fluo-4 AM (Dojindo Laboratories) or by Fura-2 AM. H9c2 (2-1) cells were incubated with 5 μM Fluo-4 AM or 3 μM Fura-2 AM in the dark at 37°C for 30 min. The loaded cells were then washed three times with Hank's Balanced Salt Solution (HBSS) and kept in HBSS for another 30 min to allow de-esterification of calcium indicators in cells.

The resting $[Ca^{2+}]_i$ fluorescence indicated by Fluo-4 was measured by an FV1000 laser scanning confocal microscope (Olympus). The data were collected and analyzed with FluoView 1.7a software (Olympus). The Ca^{2+} fluorescence indicated by Fura-2 was measured as fluorescence ratios (excitation at 340 and 380 nm; emission at 510 nm) from single cells using an Olympus IX71 inverted fluorescence microscope (Olympus) and a Luca EMCCD camera and collected at 2 s intervals. The data were recorded and analyzed by MetaFluor® Fluorescence Ratio Imaging System (Molecular Devices).

2.11 | Recombinant lentivirus

The Open Reading Frame of Kir2.1 was inserted into the MCS sites of pHBLV-CMV-MCS-3FLAG-EF1-ZsGreen-T2A-PURO to generate

lentiviral vector overexpression of Kir2.1 (Hanbio Biotechnology). The lentiviral vectors mediated Kir2.1 knockdown were generated by inserting three shRNA sequences target for Kir2.1, respectively, to pHBLV-U6-MCS-CMV-ZsGreen-PGK-PURO (Hanbio Biotechnology). To generate lentiviruses, the lentiviral vectors and packaging vectors were cotransfected into 293T cells. Cells were lysed after good transfection, and extracts were subjected to Western blot analysis.

2.12 | Western blotting

Proteins from samples of LV tissue or H9c2 (2-1) cells were loaded on 12% acrylamide gels. After electrophoretic transfer, the nitrocellulose membranes were incubated overnight at 4°C with primary antibodies against Kir2.1 (dilution 1:1000, rabbit monoclonal; Abcam), Synapse-associated protein-97 (SAP97, DLG1, dilution 1:1000, rabbit polyclonal; ABclonal), phosphorylated protein kinase A (p-PKA, dilution 1:500, rabbit polyclonal; ABclonal), PKA (dilution 1:1000, mouse monoclonal; ABclonal), Kir6.1 (KCNJ8, dilution 1:1000, rabbit polyclonal; Proteintech), and AKAP5 (dilution 1:1000, rabbit polyclonal; ABclonal). GAPDH (dilution 1:5000, rabbit/mouse monoclonal; ABclonal) was used as the loading control in each case. The secondary antibody is goat antirabbit or goat antimouse IgG (ABclonal). Quantification was performed using Image J.

2.13 | Molecular docking

The crystal structure of Kir2.1 (PDB ID 1U4F), pore-forming isoforms Kv4.3/4.2 underlying I_{to} fast component currents (PDB ID 2I2R and 7F0J, respectively), and the voltage-gated sodium channel Nav1.5 underlying I_{Na} (PDB ID 6UZ3) were downloaded from RCSB Protein Data Bank. There is no appropriate crystal structure of Cav1.2 (voltage-dependent L-type calcium channel subunit alpha-1c) in PDB, we applied the AlphaFold protein structure database (Alphafold Q13936). The 3D structure of Tet was downloaded from NCBI PubChem Compound. The binding pockets for Kir2.1 were predicted using PYVOL, the largest predicted spheres were selected as the most possible binding sites. Then molecular docking study was performed using Autodock 4.0. Every docking experiment generated at least 13 docking poses. The top rank pose was chosen as the optimal binding pose according to docking scores.

2.14 | Statistical analysis

Quantitative data were presented as the mean ± SEM and analyzed using the least significant difference or Games-Howell tests of ANOVA (analysis of variance). The statistical difference in the occurrence frequency for an individual type of arrhythmias between groups was assessed using the χ^2 (chi-square) test of two variables. Statistical differences were considered significant when the p value was <.05.

2.15 | Nomenclature of targets and ligands

Key protein targets and ligands in this article are hyperlinked to corresponding entries in http://www.guidetopharmacology.org, the common portal for data from the IUPHAR/BPS Guide to PHARMACOLOGY,[24] and are permanently archived in the Concise Guide to PHARMACOLOGY 2019/20 (Alexander et al., 2019).[25]

3 | RESULTS

3.1 | Tetramisole selectively increases the I_{K1} current in ARVMs

The Ba^{2+}-sensitive currents at the end of each 500-ms step pulse were considered the steady-state I_{K1} currents. As Figure 1 showed, tetramisole at 1–100 μmol/L enhanced both the inward and outward components of I_{K1} in a concentration-dependent manner. The maximal efficacy appeared at 30 μmol/L, with a mean increase of 66.4% in the inward current (Figure 1C, at −120 mV, $p < .05$) and 60.4% in the outward current (Figure 1D, at −50 mV, $p < .01$). Tet at 100 μmol/L showed a minor weak trend on I_{K1} enhancement than that at 30 μmol/L. The mean value of membrane capacitances is shown in Table S1.

3.2 | Tetramisole does not affect other ion channels and Na/Ca exchanger

3.2.1 | L-type Ca^{2+} current (LTCC, $I_{Ca\text{-}L}$)

The typical trace recordings and I–V curves of $I_{Ca\text{-}L}$ are shown in Figure 2A. $I_{Ca\text{-}L}$ traces were recorded using 500-ms voltage steps from a holding potential of −40 mV to voltages between −40 and 50 mV by a 10-mV step. The I–V curves of $I_{Ca\text{-}L}$ in the absence and presence of Tet are almost overlapped. Tet at 1–30 μmol/L had no significant effect on $I_{Ca\text{-}L}$ ($n = 6$, $p > .05$).

3.2.2 | Voltage-gated Na^+ channel

I–V curves of I_{Na} were recorded by 200 ms depolarizing pulses from the holding potential of −110 mV to voltages between −100 mV and 30 mV by a 5-mV step. Tet at 1–30 μmol/L had no effect on I_{Na} (Figure 2B, $N = 6$, $p > .05$).

3.2.3 | I_{to} and I_{Ksus} currents

The method used for resolving I_{to} and I_{Ksus} was modified to that described previously.[26] I_{to} and I_{Ksus} were elicited by 500 ms voltage steps from a holding potential of −40 mV to voltages between −40 and 80 mV by a 10-mV step. Figure 2C showed that there was no

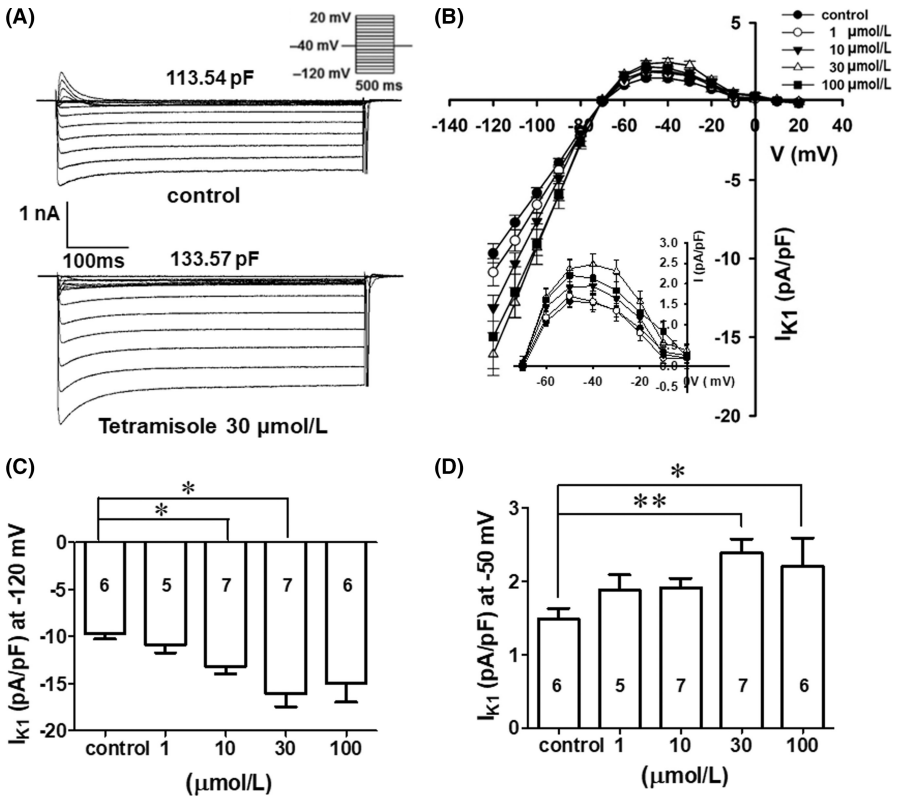

FIGURE 1 Tet increased I_{K1} current in adult rat ventricular myocytes. (A) I_{K1} current traces were recorded at a holding potential of −40 mV and 500 ms clamp voltage steps ranging from −120 to 20 mV. (B) Current–voltage (I–V) curves for I_{K1} before and after application of Tet at different concentrations (1, 10, 30, and 100 μmol/L). Embedded expanded plots for the outward component of I_{K1} from (B). Both the inward and outward components of I_{K1} were increased by Tet. All currents were normalized for cell capacitance. (C) The effect of Tet on outward components of I_{K1} at −120 mV. (D) The effect of Tet on outward components of I_{K1} at −50 mV. N, numbers embedded in the charts; Tet, tetramisole. Values are presented as the mean ± SE. $^{*}p < .05$; $^{**}p < .01$.

significant difference between the absence and the presence of 1–30 μmol/L Tet ($n = 6$, $p > .05$).

3.2.4 | Na/Ca exchanger current

The I_{NCX} current was measured with a ramp voltage clamp pulse depolarized from a holding potential of −40 to 60 mV, then hyperpolarized to −120 mV at a rate of 90 mV/s (Figure 2D). After the application of $NiCl_2$ (5.0 mmol/L), the current decreased in both the inward and the outward directions. I_{NCX} is defined as Ni^{2+}-sensitive current. Tet at 1–100 μmol/L had no effect on I_{NCX} ($n = 6$, $p > .05$).

3.3 | Tetramisole hyperpolarizes the RP and moderately shortens the APD

The effects of Tet on RP and APs in ARVMs are shown in Figure 3. At the current clamp mode, APs were triggered by injection currents (Figure 3A, 2-ms pulse width, twice of threshold at 1 Hz). In the presence of 1–100 μmol/L Tet, RP was hyperpolarized, and APD was moderately shortened in a dose-relative manner. At 30 μmol/L, Tet hyperpolarized the RP from −74.1 ± 2.1 mV (baseline) up to −79.8 ± 1.7 mV (Figure 3B, $p < .05$). Meanwhile, the APD_{90} was shortened from 37.4 ± 4.4 ms (baseline) to 25.2 ± 3.2 ms (Figure 3C, $p < .05$). Tet had no significant effect on APD_{50} and APA (Figure 3C,D). Considering the importance of I_{K1} in maintaining RP and terminal repolarization of AP, the effects of tetramisole on RP and APD highly fit the profile of a specific I_{K1} agonists.

3.4 | Tetramisole prevents acute ischemic arrhythmias either in 3-min preexposure setting or 10-day pretreatment

Acute MI-induced tachyarrhythmias usually occurred 5–6 min postcoronary occlusion and intensively appeared at 9–12 min (Figure 4Aa). So, 15 min MI was set as the model criteria. The cases with spontaneous arrhythmia were weeded out. In the setting of 3 min preexposure, Tet significantly reduced or even eliminated ventricular arrhythmias both in episode number and duration compared with the saline control. In detail, 92.3% (12 out of 13) of rats developed VT, and 84.6% (11/13) developed VF post-MI. The duration of VT and VF were 59.4 ± 17.7 s and 5.6 ± 1.6 s, respectively. Preexposure with 0.54 mg/kg Tet exhibited the most striking antiarrhythmic effects as evidenced by reduction in the episodes of PVC (from 134 ± 23 to 16 ± 7, $p < .01$), the duration (8.1 ± 5.9 s, $p < .01$) and incidence (44.4%, $p < .05$) of VT, and the duration (0 s, $p < .05$) and incidence (0%, $p < .01$) of VF. The effects could be largely counteracted by 7.5 μg/kg chloroquine, a relatively specific I_{K1} blocker at low dosage ($p < .05$ or $p < .01$). All these data suggest that the antiarrhythmic effects of Tet are mediated by I_{K1} activation (see the details in Figure 4A).

Tet 10-day pretreatment could inhibit ventricular arrhythmia induced by acute myocardial ischemia (Figure 4B). Tet at 0.54 mg/kg/day strikingly reduced the duration of VT (from 42.7 ± 13.7 to 6.5 ± 2.4, $p < .01$) and VF (8.2 ± 3.4 to 0, $p < .01$) and the incidence of VF (from 85.7% to 0, $p < .01$). The anti-arrhythmic effect could be largely abolished by chloroquine ($p < .05$). Native I_{K1} channels in the ventricles predominantly comprise Kir2.1 (KCNJ2) subunits.

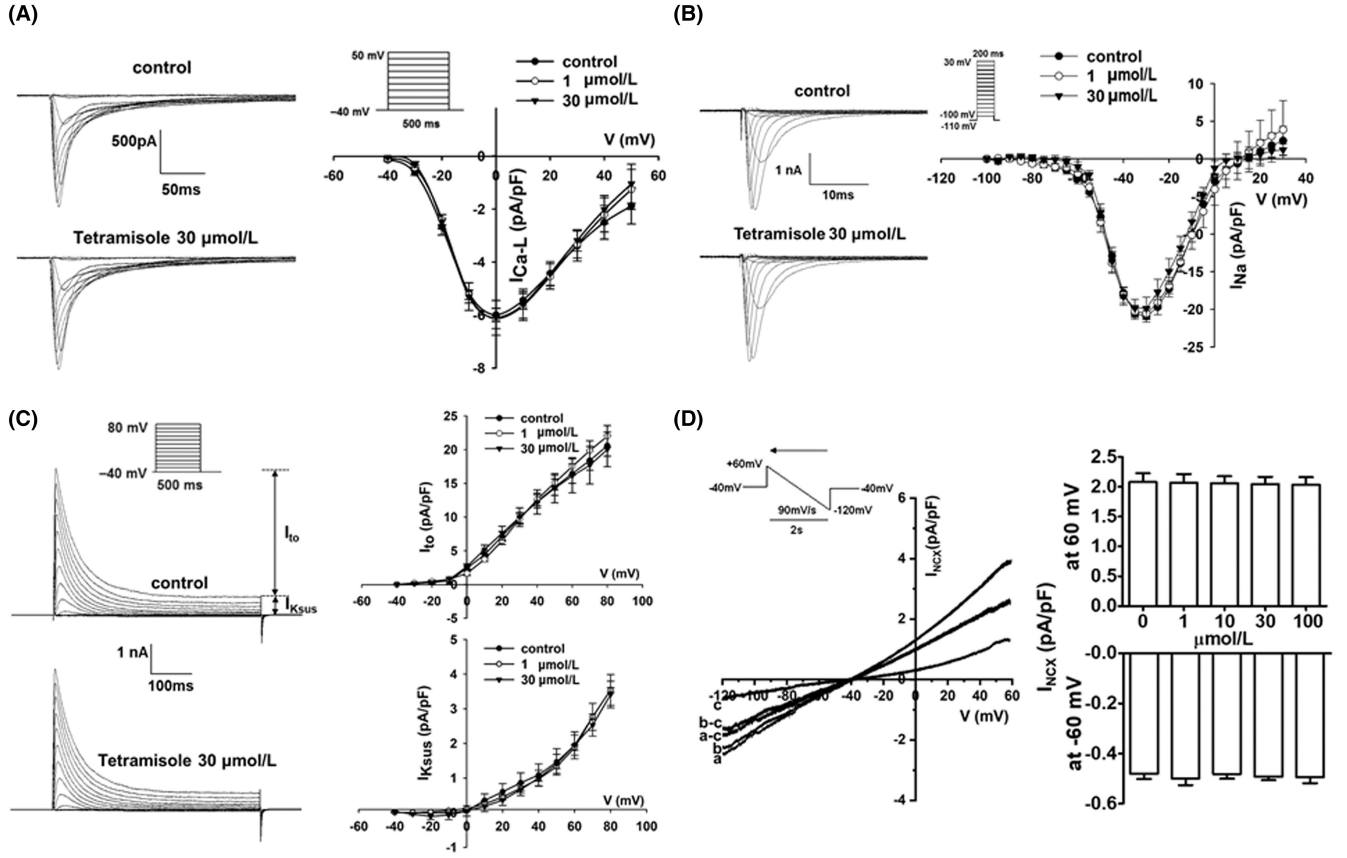

FIGURE 2 Tet had no effects on other channels and Na/Ca exchanger. (A) $I_{Ca\text{-}L}$ traces were recorded using 500 ms voltage steps from a holding potential of −40 mV to voltages between −40 and 50 mV by a 10-mV step. Tet had no significant effect on $I_{Ca\text{-}L}$. (B) I_{Na} was recorded by 200-ms depolarizing pulses from the holding potential of −110 mV to voltages between −100 and 30 mV by a 5-mV step. Tet had no effect on I_{Na}. (C) I_{to} and I_{Ksus} were recorded by 500-ms voltage steps from a holding potential of −40 mV to voltages between −40 and 80 mV by a 10-mV step. I_{to} refers to the difference between the peak outward current and the steady-state current at the end of a pulse. I_{Ksus} was the difference between the steady-state current and the holding current in the same recording. Tet had no effect on I_{to} and I_{Ksus}. (D) The I_{NCX} current was measured with a ramp voltage clamp pulse depolarized from a holding potential of −40 mV to 60 mV, then hyperpolarized to −120 mV at a rate of 90 mV/s. Tet had no effect on I_{NCX}. a: Control; b: 30 μmol/L tetramisole; c: 5.0 mmol/L $NiCl_2$; a–c: baseline I_{NCX} (Ni^{2+}-sensitive current); b, c: I_{NCX} postapplication of Tet. $n = 6$ in each treatment. Tet, tetramisole. Values are presented as the mean ± SE.

Western blot data showed that pretreatment with Tet (0.54 mg/kg/day) for 10 days significantly increase the expression of Kir2.1 channel protein ($p < .01$), which could be reversed by chloroquine, an I I_{K1} blocker ($p < .05$).

All these data suggested that the anti-arrhythmic effects of Tet are mediated by I_{K1} activation.

3.5 | Tetramisole improves Iso-induced cardiac remodeling in vivo

3.5.1 | Echocardiography

Echocardiographic observation demonstrated the typical characteristics of concentric hypertrophy and enhanced pumping function (Figure 5A; Table 1). Post-10 days of Iso infusion, IVSd, IVSs, EF, and FS were increased ($p < .01$); LVIDs ($p < .05$) were reduced compared with control rats. Tet treatment prevented the thickening of interventricular septum, increased LV volume ($p < .05$), and normalized cardiac pumping function ($p < .01$). The effect could be largely reversed by the I_{K1} antagonist, chloroquine ($p < .01$ or $p < .05$). Tet (0.54 mg/kg/day) in present study or chloroquine (7.5 μg/kg/day)[14] per se had no significant effects on cardiac structure or function.

3.5.2 | Morphological features

Cardiac remodeling is a response to damages characterized by myocardial hypertrophy and interstitial fibrosis. Transverse sections of the LV were stained with HE. As shown in Figure 5B, compared with controls, the cardiac myofibers in Iso-infused rats are disorganized and hypertrophic, with a certain degree of cell necrosis and relatively light staining of the cytoplasm. In tetramisole-treated rats, cardiac myofibers are better arranged with normalized size. I_{K1} channel blocker chloroquine counteracted the protection, indicating that the antiremodeling effect of Tet is mediated by I_{K1} activation.

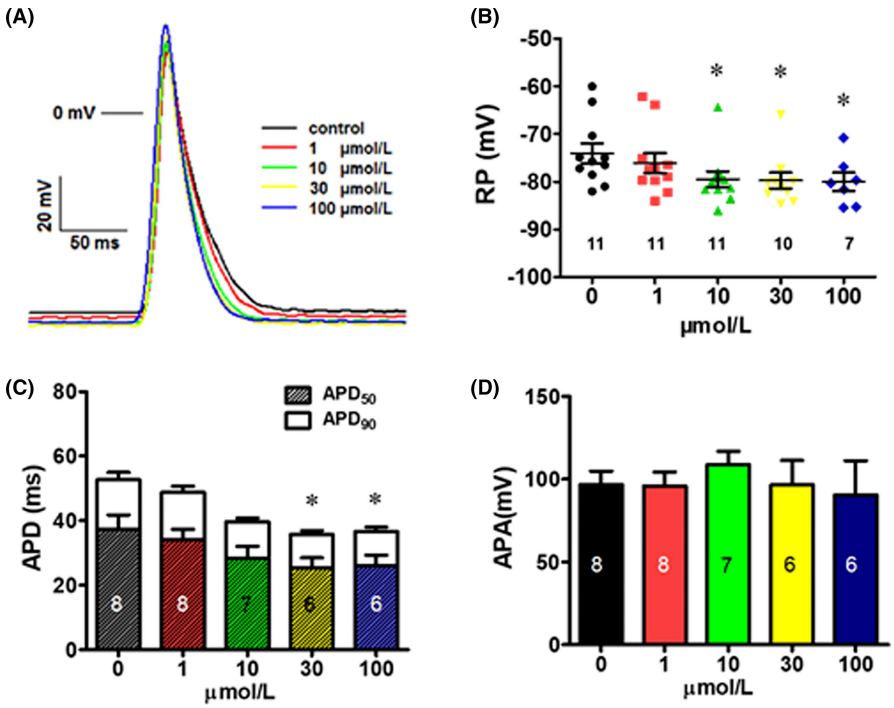

FIGURE 3 Tet hyperpolarized the RP and shortened the APD_{90} in a dose-relative manner in isolated adult rat ventricular myocytes. (A) Representative AP traces before and after Tet application. (B) 10–100 μmol/L Tet hyperpolarized RP. (C) 30 and 100 μmol/L Tet shortened APD_{90} but had no significant effect on APD_{50}. (D) Tet had no significant effect on APA. APD_{50} and APD_{90}, APD at 50% and 90% of repolarization, respectively. *N*, numbers embedded in the charts. Values are presented as the mean ± SE. *$p < .05$ versus control (0 μmol/L). AP, action potential; APD, action potential duration; RP, resting potential; Tet, tetramisole.

After 10 days of Iso infusion, rat hearts exhibited significant fibrosis, validated by increased collagen deposition (Figures 5C). Tet strikingly attenuated the fibrosis ($p < .01$), and this effect was largely abolished by chloroquine ($p < .01$). Tet (0.54 mg/kg/day) in present study or chloroquine (7.5 μg/kg/day)[14] per se had no significant effects on cardiac structure.

3.6 | Tetramisole prevents Iso-induced intracellular Ca^{2+} overload in cardiomyocytes

In H9c2 (2-1) cardiomyocytes, the Ca^{2+} imaging data showed that 1 μmol/L Iso-induced electrical remodeling as evidenced by higher $[Ca^{2+}]_i$ compared with controls ($p < .01$) (Figure 6). Tet at 10 or 30 μmol/L alleviated Iso-induced $[Ca^{2+}]_i$ overload ($p < .01$), and the effect could be reversed by $BaCl_2$ ($p < .01$), respectively. Notably, without Iso stimulus, Tet at 1–100 μmol/L had no effect on intracellular $[Ca^{2+}]_i$, suggesting that the protection of Tet against Ca^{2+} overload is compensation for Ca^{2+} dyshomeostasis in remodeled cardiomyocytes.

In isolated ARVMs, 30 μmol/L tetramisole showed significant cardioprotection on Iso-induced Ca^{2+} overload whether by acute or chronic infusion ($p < .05$ or $p < .01$), and the effect could be reversed by $BaCl_2$ ($p < .01$). Please see the details in Figure S1.

3.7 | Tetramisole upregulates Kir2.1 and SAP97 and inhibits PKA-AKAP5 signaling in cardiomyocytes upon Iso infusion

Native I_{K1} channels in the ventricles predominantly comprise Kir2.1 (KCNJ2) subunits. SAP97 is a membrane-associated guanylate kinase (MAGUK) scaffolding protein that contributes to the function, localization, and forward (toward the plasma membrane) trafficking behavior of the Kir2.1 channel.[27,28] In normal H9c2 (2-1) cardiomyocytes, Tet significantly upregulated the expression of SAP97 (Figure 7B, $p < .01$) in parallel with that of Kir2.1 (Figure 7A, $p < .01$ or $p < .05$). The maximal efficacy appeared at 30 μmol/L with Kir2.1 augmentation of 56.6 ± 0.15% and SAP97 augmentation of 57.2 ± 0.09% compared with control. In remodeled H9c2 (2-1) cells, Iso downregulated Kir2.1 ($p < .05$). Tet at 10 or 30 μmol/L normalized the expression of Kir2.1 ($p < .05$ or $p < .01$), and the effects were largely reversed by I_{K1} blocker $BaCl_2$. Although both Iso and $BaCl_2$ downregulated the expression of Kir2.1, Iso had no significant effect on SAP97 whereas the latter counteracted the effects of Tet on SAP97 ($p < .05$). Iso might downregulate Kir2.1 in a SAP97-independent pathway. We further observed the interactions involving SAP97 and Kir2.1 by lentivirus-driven knockdown or overexpression of Kir2.1 in H9c2 (2-1) cells. As shown in Figure S2, compared with negative control, neither Kir2.1 knockdown nor Kir2.1 overexpression had effects on the expression of SAP97.

ATP-sensitive K^+ channel (K_{ATP}) and I_{K1} channels are both members of the inward rectifier potassium (Kir) channel family and, respectively, constituted by Kir2.x and Kir6.x subunits.[29] K_{ATP} is documented involved in ventricular remodeling, and K_{ATP} channel agonists improved cardiac structural remodeling and dysfunction.[30,31] To rule out the possibility that the cardioprotective features of Tet are mediated by activation of K_{ATP}, the expression of Kir6.1, the predominant subunit of K_{ATP}, was observed in Iso-infused H9c2 (2-1) cells. The present results suggested that 1–100 μmol/L Tet had no significant effects on Kir6.1 in neither Iso stress nor control condition (Figure 7C).

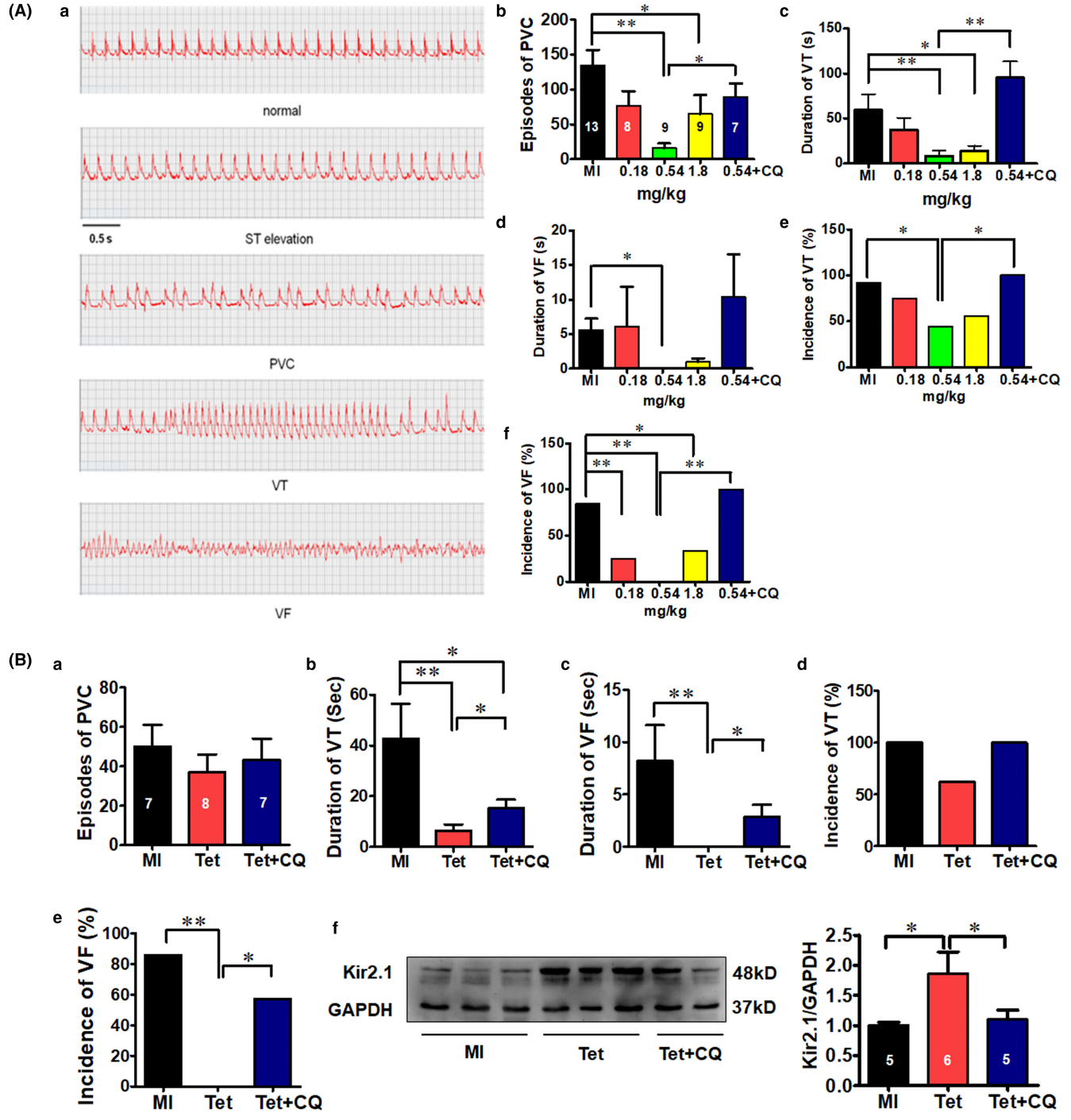

FIGURE 4 Tet prevented acute ischemic arrhythmias in rats in vivo. (A) Tet preexposure. (a) The representative electrocardiogram illustrating multiple ventricular arrhythmias. The elevation of ST segment indicates the establishment of cardiac ischemia. The effects of Tet on the episodes of PVC (b), the duration of VT (c) and VF (d), the incidence of VT (e) and VF (f). Tet at 0.54 mg/kg exerted the optimal anti-arrhythmic efficacy, which could be largely reversed by I_{K1} blocker chloroquine. (B) Pretreatment with Tet (0.54 mg/kg/day) for 10 days. The effects of Tet on episodes of PVC (a), the duration of VT (b) and VF (c), the incidence of VT (d) and VF (e). (f) Tet upregulated the expression of Kir2.1 in rat ventricle, and the effect was largely reversed by chloroquine. The results were normalized with MI ratio, respectively. CQ, chloroquine; PVC, premature ventricular contraction; Tet, tetramisole; VT, ventricular tachycardia; VF, ventricular fibrillation. Values are presented as the mean ± SE. *N*, numbers embedded in the charts. $^{*}p < .05$; $^{**}p < .01$.

β-adrenergic receptors (β-AR) stimulation in the heart could activate the cAMP/PKA pathway. Phosphorylation of PKA plays key roles in the progression of cardiac remodeling and HF. Figure 7D shows that 1 μmol/L Iso-induced hyperphosphorylation of PKA ($p < .05$), and the effects were reversed by 30 μmol/L Tet ($p < .01$). To further clarify how Tet inhibits phosphorylation of PKA, we detected the expression of A-kinase-anchoring protein 5 (AKAP5, also known as AKAP150 in rats) is a widely expressed

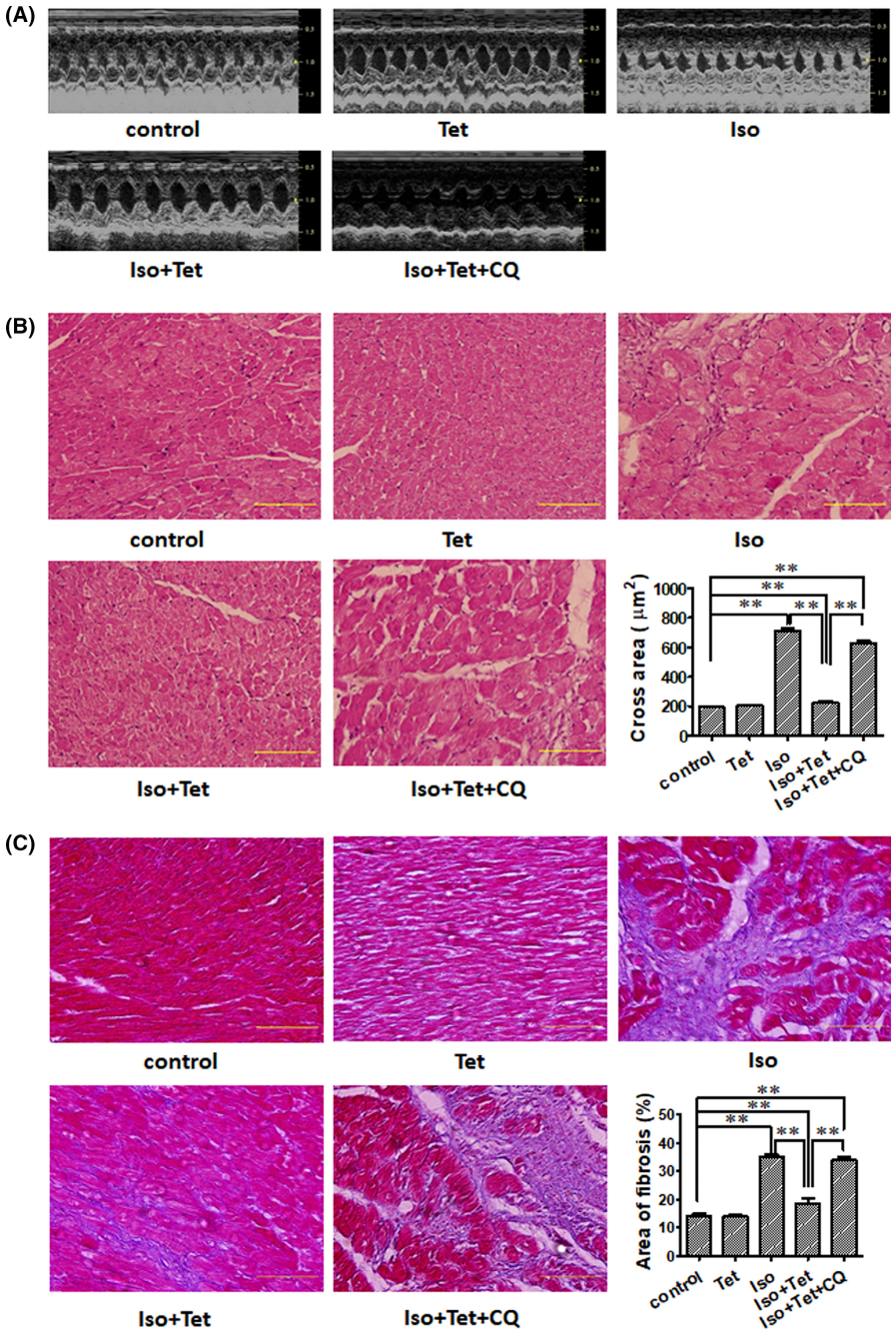

FIGURE 5 Tet attenuated cardiac remodeling induced by 10 days of Iso exposure in rats in vivo. (A) The representative echocardiographic images. (B) Hematoxylin and eosin staining of transverse left ventricle (LV) sections (400×) and statistical results of the cross-sectional area of myofibers in different groups. Scale bars = 100 μm. $N = 100$ in each group. (C) Collagen deposition in rat LV was observed by Masson's trichrome staining (400 ×) and statistical results showing the percentage of fibrotic area in total area under each high power field. Cardiomyocytes and collagen fibers were stained red and blue, respectively. Scale bars = 100 μm. $N = 8$ in each group. CQ, chloroquine; Iso, isoproterenol; Tet, tetramisole. Data are presented as mean ± SEM. $^{**}p < .01$.

anchor protein that binds to the regulatory subunit of protein kinase A (PKA). Figure S3B shows that 10 and 30 μmol/L Tet downregulated the expression of AKAP5 ($p < .01$), and 1 μmol/L $BaCl_2$ counteracted the effect of Tet at 30 μmol/L ($p < .05$). Notably, in the absence of Iso stress, 1–100 μmol/L Tet had no significant effects on the expression of AKAP5 and the phosphorylation of PKA (Figure 7D; Figure S3A).

3.8 | Tetramisole selectively binds to Kir2.1

Molecular docking was performed to predict the possible interaction between Tet and the most important ion channel protein contributing to ventricular action potentials.[32] Tet was found to be formed a special S…O bond at residue Glu224 and an alkyl–π interaction at residue Arg260 from Chain B of Kir2.1 (Figure 8). Further docking study showed that a Pi–Pi interaction was observed between the benzene ring of Tet and PHE 98 residue of Kv4.3 (Figure S4A), but there was no binding activity between Tet with Kv4.2, Nav1.5, or Cav1.2 (Figure S4B–D).

4 | DISCUSSION

The novel findings in the present study include (1) by drug repurposing, big data analysis, molecular docking, and experimental evidence,

TABLE 1 Echocardiographic parameters in Iso-treated rats (mean ± SEM)

	n	IVSd (mm)	IVSs (mm)	LVIDd (mm)	LVIDs (mm)	LVPWd (mm)	LVPWs (mm)	EF (%)	FS (%)
Control	7	1.64 ± 0.14	2.72 ± 0.25	5.21 ± 0.25	2.88 ± 0.10	1.62 ± 0.15	2.64 ± 0.12	80.7 ± 2.1	44.3 ± 2.2
Tet	6	1.55 ± 0.03	2.81 ± 0.24	5.71 ± 0.25	2.80 ± 0.32	1.70 ± 0.09	2.94 ± 0.09	85.8 ± 3.6	51.3 ± 4.3
Iso	7	2.20 ± 0.15**	3.78 ± 0.32$^{**,\#}$	4.81 ± 0.43	1.94 ± 0.29$^{*,\#}$	1.87 ± 0.11	3.07 ± 0.33	92.4 ± 1.8$^{**,\#}$	60.1 ± 3.1$^{**,\#}$
Iso + Tet	6	1.93 ± 0.10	3.10 ± 0.09	5.50 ± 0.42	2.93 ± 0.38	1.89 ± 0.15	2.91 ± 0.15	82.2 ± 4.0	47.0 ± 4.4
Iso + Tet + CQ	6	2.20 ± 0.13**	4.20 ± 0.18$^{**,\#\#}$	5.49 ± 0.15	2.20 ± 0.22$^{\#}$	1.93 ± 0.08*	3.10 ± 0.15	92.2 ± 2.0$^{**,\#}$	60.0 ± 3.4$^{**,\#}$

Note: The dose of Tet is 0.54 mg/kg/day, and the dose of chloroquine is 7.5 μg/kg/day.

Abbreviations: CQ, chloroquine; EF, ejection fraction; FS, fractional shortening; Iso, isoproterenol; IVSd, interventricular septum end-diastolic thickness. IVSs, interventricular septum end-systolic thickness; LVIDd, left ventricular dimension in end-diastole; LVIDs, left ventricular dimension in end-systole; Tet, tetramisole.

$^{*}p < .05$; $^{**}p < .01$ versus control.

$^{\#}p < .05$.

$^{\#\#}p < .01$ versus Iso + Tet.

Tet was identified as a specific I_{K1} agonist in rat, and (2) I_{K1} channel is a promising target for the regulation of intracellular calcium overload that linking cardiac remodeling and arrhythmias.

4.1 | Activation of I_{K1} is a new regulatory strategy on intracellular Ca^{2+} dyshomeostasis associated with cardiac remodeling and arrhythmogenesis

Cardiac remodeling generally encompasses two components, structural and electrical remodeling. Electrical remodeling, such as alterations in ion channels or Ca^{2+} cycling, may constitute the electrophysiological basis underlying arrhythmogenesis. Amelioration of electrical remodeling might be an effective strategy against HF and associated arrhythmia. Calcium dyshomeostasis, especially pathologic elevation of intracellular Ca^{2+} (Ca^{2+} overload), is a pivotal electrical event linking arrhythmogenesis and cardiac remodeling.[14,33] β-AR stimulation increases calcium influx through LTCC,[34] phosphorylates CaMKII and cAMP-dependent PKA that facilitates calcium leakage from RyRs, concurrently reducing Ca^{2+} uptake into the SR by downregulating SERCA2.[14,35] All these changes ultimately lead to the intracellular Ca^{2+} overload. Furthermore, in cardiac hypertrophy and HF, prolongation of APD, downregulation of I_{K1} channel, enhanced depolarization drive, and reduced repolarization reserve are hallmarks of electrical remodeling.[4,14,36,37] From our previous work, the RP depolarization, I_{K1} reduction, and APD prolongation were well recognized during the early stage of simulated ischemia in ARVMs in vitro.[3] Downregulation of I_{K1} also contributes to APD prolongation and terminal repolarization of AP. Depolarized RP and prolonged APD facilitate the opening of LTCC thus promoting intracellular Ca^{2+} accumulation.[38] We have proven that in conditions of ischemic membrane damage or adrenergic stimulation, Ca^{2+} overload, and APD prolongation may initiate delayed afterdepolarization (DAD), which underlies the genesis of triggered arrhythmias.[3,12] Elevation of cardiomyocyte $[Ca^{2+}]_i$ elicits a series of biochemical signals through multifaceted Ca^{2+}-activated enzymes, such as Ca^{2+}–/calmodulin-dependent protein kinase II (CaMKII). Activated CaMKII phosphorylates multiple ion channels and Ca^{2+} handling proteins, in turn, aggravating intracellular Ca^{2+} dyshomeostasis.[14]

Ca^{2+} also produces voltage-dependent blockade of I_{K1}. In Guinea pig ventricular myocytes, transient increase of $[Ca^{2+}]_i$ during the AP lead to inhibition of I_{K1} outward current by decreasing the open probability of the channel.[39,40] In HF, I_{K1} is observed reduced by elevated diastolic Ca^{2+} in HF which provides a paradigm for Ca^{2+}-dependent modulation of RP.[41]

By enhancing I_{K1}, Tet reversed RP depolarization and APD prolongation, consequently inhibiting cardiac Ca^{2+} overload. It is benign to diminish the onset of DAD/EAD and Ca^{2+}-dependent transcriptional pathway for cardiac hypertrophy.

Similar to zacopride, Tet per se had no effect on LTCCs or I_{NCX}. The regulation of calcium homeostasis is probably I_{K1}-dependent. The convincing data came from the coapplication of I_{K1} antagonist

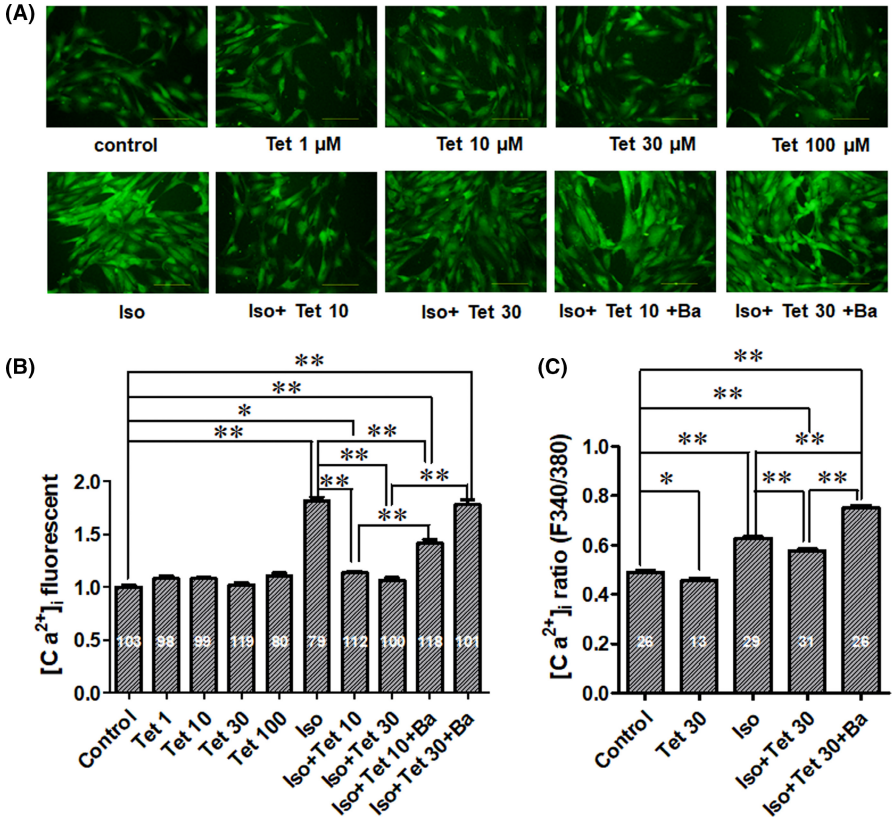

FIGURE 6 Tet attenuated Iso-induced $[Ca^{2+}]_i$ overload in H9c2 (2–1) cells. (A) Fluorescent images of Fluo-4/AM loaded H9c2 (2-1) cardiomyocytes. Magnification: 200×. Bars represent 100 μm. (B) In Fluo-4/AM loaded H9c2 (2-1) cardiomyocytes, Tet treatments attenuated Iso-induced intracellular calcium overload, and the effects could be reversed by I_{K1} blocker $BaCl_2$. (C) In Fura-2/AM loaded H9c2 (2-1) cardiomyocytes, 30 μmol/L Tet attenuated Iso-induced intracellular calcium overload, and the effects could be reversed by I_{K1} blocker $BaCl_2$. Ba, $BaCl_2$; Iso, isoproterenol; *N*, numbers embedded in the columns; Tet, Tetramisole. Values are presented as the mean ± SEM. $^*p < .05$; $^{**}p < .01$.

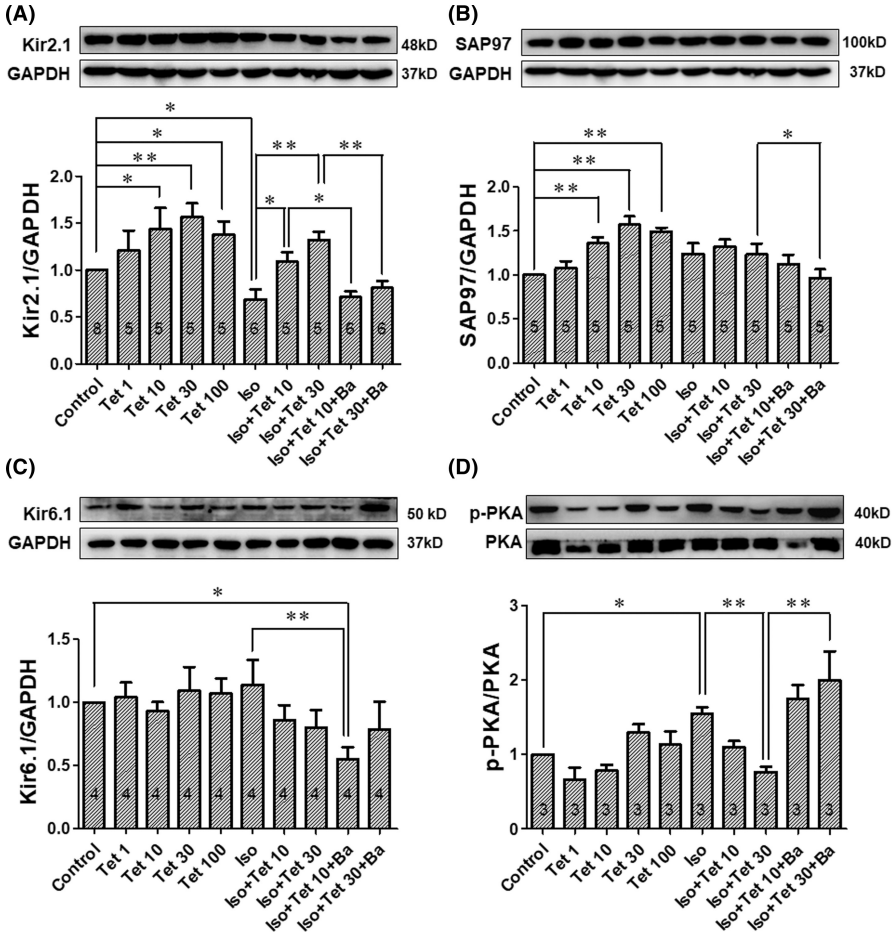

FIGURE 7 Effects of Tet on Kir2.1, SAP97, Kir6.1, and PKA signaling in H9c2 (2–1) cells. (A) Tet upregulated Kir2.1 channel expression. (B) Tet upregulated SAP97 expression. The representative blots in A&B derived from the same gel but different nitrocellulose membranes according to a certain molecular range. (C) Tet had no effects on Kir6.1 channel expression. (D) Tet inhibited the phosphorylation of PKA in Iso-infused H9c2 (2-1) cells. PKA activity is expressed as the ratio of phosphorylated PKA to total PKA. Ba, $BaCl_2$; *N*, numbers embedded in the columns; Iso, isoproterenol; Tet, Tetramisole. Values are presented as the mean ± SEM. $^*p < .05$; $^{**}p < .01$.

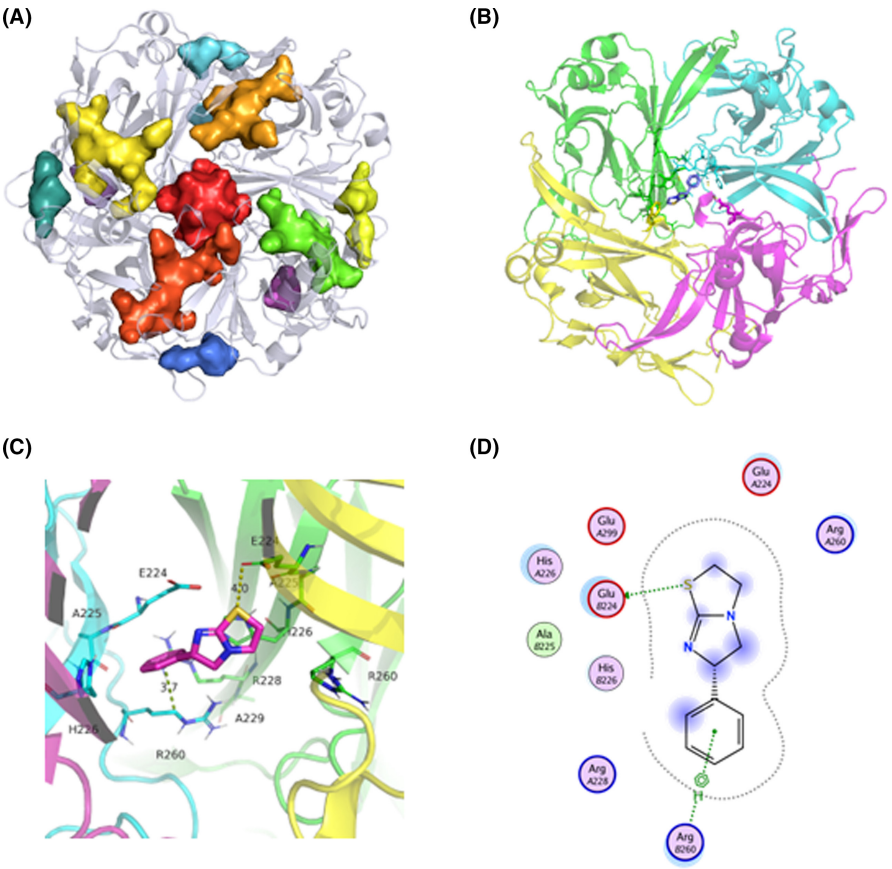

FIGURE 8 Molecular docking to predict the binding of Tet to Kir2.1. The ligand (Tet) is shown in stick mode. The receptor is shown in cartoon and surface models. (A) The binding pocket of the ligand targeting Kir2.1. The red region was the most possible binding pocket of ligand (tetramisole) and was located at the axis center of the tetramer. (B) Overview of Tet and Kir2.1 complex. (C) Demonstration of Tet docking into Kir2.1. (D) A special S...O interaction has been observed between the lone pair electrons of sulfur atom of Tet and carbonyl oxygen of Glu224 from chain B. In addition, an alkyl–π interaction has been also observed between the side chain of Arg260 from Chain B and the benzene ring of tetramisole. The top pose docking score is −8.5631 kcal/mol.

$BaCl_2$, or chloroquine. $BaCl_2$ in vitro or chloroquine in vivo blunted the cardioprotection of Tet. Specifically, Tet only attenuated Ca^{2+} overload in cardiomyocytes upon Iso stress, compared with no effect in normal myocytes. The I_{K1} channel might be a novel target for maintaining calcium homeostasis.

4.2 | Tetramisole showed high selective affinity with Kir2.1 and might upregulate I_{K1} by facilitating Kir2.1 forward trafficking

In the present study, an in silico study molecular docking was performed to clarify the pharmacological selectivity of the ligand (Tet) with the receptor (Kir2.1). Tet showed binding activity with Kir2.1 and Kv4.3 but had no interaction with Kv4.2, Nav1.5, or Cav1.2 channel protein. Considering that $I_{to,f}$ channels are constituted by both Kv4.2 and Kv4.3 in rodent ventricles and Tet had no significant on I_{to} current by patch clamp technique, Tet might be a selective pharmacological tool in regulation of Kir2.1 channel.

The trafficking of channel proteins might determine the channel density. Forward trafficking allows correctly folded nascent Kir2.1 protein trafficking toward and anchoring at the plasma membrane, where the channel plays biophysical roles. Upon removal from the plasma membrane, Kir2.1 channel proteins can enter the lysosome degradation pathway named backward trafficking.[42] MAGUK proteins, serve as regulatory partners (channel interacting proteins, ChIPs) to the channel proteins and are characterized by sharing multiple protein–protein interaction domains, including PDZ (postsynaptic density protein-95), Drosophila disc large tumor suppressor (Dlg1), and SH3 domains (SRC Homology 3 Domain).[27] In hearts, SAP97 is the most well-characterized MAGUK protein which regulates Kir2.1 localization, forward trafficking, and formation of signaling complexes.[28,43,44] SAP97 knockdown in ventricular myocytes resulted in a downregulation of Kir2.1 and severe disruption of Kir2.1 localization. Vaidyanathan et al. demonstrated that silencing SAP97 decreased I_{K1} density which was likely due to a decrease in the abundance of Kir2.1 channels on the membrane.[28] These alterations were associated with a prolongation of the APD which signifies arrhythmogenic propensity.[43] Conversely, in the present study, lentivirus-mediated Kir2.1 overexpression or knockdown had no effects on the expression of SAP97. Tet upregulated the expression of SAP97 in a dose-relative manner, which is in line with the effects of Tet on Kir2.1 current and expression. All these data support that Tetramisole increases cardiac Kir2.1 by positively regulating SAP97. Upregulation of SAP97 may facilitate the forward trafficking of Kir2.1 and increase the membrane conductance of Kir2.1 which well explain the hyperpolarization of RP and acceleration of terminal repolarization of AP. A notable observation indicated that Iso stimulation did not alter the expression of SAP97 although Kir2.1 was downregulated. So, Iso might inhibit Kir2.1 by a SAP97-independent pathway. A low dose of $BaCl_2$ (e.g., 1 μmol/L) and chloroquine (0.3 μmol/L or 7.5 μg/kg in vivo) are used as a relative specific blocker of the I_{K1} channel. Our previous work showed that 1 μmol/L $BaCl_2$ or 0.3 μmol/L chloroquine

downregulated the expression of SAP97 in cardiomyocytes, parallel to the inhibition of the Kir2.1 channel. It partly elucidated why $BaCl_2$ or chloroquine counteracted the cardioprotection of tetramisole.

4.3 | The cardioprotection of tetramisole is associated with negative regulation of PKA-AKAP5 signaling in H9c2 (2-1) cardiomyocytes

Beta-adrenergic receptor (β-AR) stimulation (such as by acute MI or Iso) could activate the cAMP-dependent PKA. PKA is considered to be a key downstream effector in cAMP/PKA signaling. Activated PKA phosphorylates multiple substrates such as LTCC, RyR2, cardiac myosin binding protein (cMyBP), and PLN, resulting in increased intracellular Ca^{2+}, the loss of excitation–contraction coupling, contraction, and relaxation dysfunction (reviewed by Saad et al., 2018).[45] In HF, the activity and expression of PKA were significantly increased compared with nonfailing hearts.[46,47] While PKA inhibition decreased cell death occurring in I/R and HF.[47–49]Although it is still a contentious issue about the exact role of PKA in cardiomyopathy, most reports showed PKA inhibition as a potential target in the treatment of cardiac hypertrophy, cardiac dilation, I/R, MI, and HF.[45]

The PKA holoenzyme is a heterotetramer consisting of two catalytic and two regulatory subunits. Phosphorylation of PKA in cardiomyocytes regulates multiple ion flux. Kir2.x channels including Kir2.1 are the substrates of PKA too. But the conditioning effect remains a matter of debate. In heterologous expression systems, activation of PKA via Iso, cAMP, or forskolin enhances the outward current of Kir2.1.[50] While in native cardiomyocytes, I_{KI} was suppressed by PKA-mediated phosphorylation in response to β1-AR stimulation.[51,52] Protein kinase A anchoring proteins (AKAPs) are a family of anchoring proteins, which are localized by binding to the regulatory subunits of the cyclic AMP-dependent PKA. It has been reported that overexpression of muscle AKAP in cardiomyocytes increased PKA-catalyzed phosphorylation of ryanodine Ca^{2+} release channels and inhibit adrenergic-induced hypertrophy.[53] AKAP5 is a membrane-bound AKAP and was involved in tethering β1-AR[54] and spatiotemporal regulating phosphorylation of PKA.[55] In the present study, Iso elicited phosphorylation of PKA and downregulation of Kir2.1 in H9c2 (2-1) cardiomyocytes, as was consistently observed in previous studies. In line with the activity of PKA, tetramisole inhibited the expression of AKAP5 in Iso-infused H9c2 (2-1) cells. The inhibition of PKA and AKAP5 by tetramisole may partially explain its activation on Kir2.1 upon Iso stimuli. All these effects could be reversed by I_{K1} blocker $BaCl_2$. These provide a possible relationship between PKA–AKAP5 association and Kir2.1 regulation. It is worthy of note that without β1-AR stimuli, Tet (at 1–100 μmol/L) is lack of significant impact on the expression of AKAP5 and PKA activation. Therefore, enhancing I_{K1} might be negative feedback that limits the PKA-mediated depolarization and calcium overload.

4.4 | Limitations and prospects

In the present study, we applied an in silico structure-based method to predict ligand–target interactions at molecular levels. The combination of drug repositioning and molecular docking might complement each other in more accurate target identification and drug discovery. But validation is necessary using in vitro binding assays, such as western blotting, immunofluorescence staining, and genetic modulation to confirm the key binding sites of the ligands to the receptor (Kir2.1).

Both loss and gain of function in cardiac I_{K1} are associated with severe arrhythmias andf even sudden cardiac death.[56,57] Loss of ventricular I_{K1} current is a hallmark of electrical alteration underlying arrhythmogenesis in human failing hearts. While a ventricular I_{K1} increase may accelerate and stabilize the reentry rotors and ventricular fibrillation dynamics.[58] Therefore, when judging an anti-arrhythmic strategy, a comprehensive understanding of mechanisms underlying certain arrhythmogenesis and drug therapy would be essential and beneficial. Based on previous and present research, we suggest that I_{K1} channel agonists and related new anti-arrhythmic drugs might be applied under conditions of automaticity and triggered arrhythmias. Further, many clinical anti-arrhythmic drugs have been revealed of potential pro-arrhythmic risks. Compared with dramatic changes by genetic manipulation, Tet and zacopride are moderate I_{K1} agonists, with limited efficacy on I_{K1} and AP. Modulating I_{K1} within the physiological range is important to minimize the pro-arrhythmic effects of anti-arrhythmic medications. The last concern is the risk of atrial arrhythmia. Gain of I_{K1} function has been deemed a risk factor for atrial arrhythmogenesis.[57,59] Because that Kir2.1 is the major isoform underlying human ventricular I_{K1} and a minor constituent in atrial I_{K1},[60] an ideal and promising anti-arrhythmic agent targeting I_{K1} should be Kir2.1-specific and of lower disturbance on atrial I_{K1}.

AUTHOR CONTRIBUTIONS

Participated in research design: Bowei Wu, Peifeng He, Qi Yu, Xuechun Lu, and Jimin Cao. Conducted experiments: Qinghua Liu, Jiaxing Sun, Yangdou Dong, Pan Li, Jin Wang, Yulan Wang, and YanwuXu. Performed data analysis: Qinghua Liu and Xinrui Tian. Wrote or contributed to the writing of the manuscript: Qinghua Liu and Jimin Cao.

ACKNOWLEDGMENTS

The authors would like to thank Xi Qiao, Lijun Zhang, and Jing Shen for their technical assistance and animal care.

FUNDING INFORMATION

This work was supported by grants from the National Natural Science Foundation of China (82170523) and the Natural Science Foundation of Shanxi Province (no. 20210302123309); Grants from the Key Laboratory of Medical Electrophysiology (Southwest Medical University), Ministry of Education of China (KeyME-2017-04); Open Fund from Key Laboratory of Cellular Physiology (Shanxi Medical University), Ministry of Education, China

(KLMEC/SXMU-201909); Key R&D Program of Shanxi Province (201903D311011); National Social Science Fund of China (21BTQ050).

DISCLOSURE

No author has an actual or perceived conflict of interest with the contents of this article.

DATA AVAILABILITY STATEMENT

Data are available on reasonable request from the authors.

ETHICS STATEMENT

This study was carried out in accordance with the recommendations of the guidelines for the Care and Use of Laboratory Animals (NIH, revised 2011), and approved by the Ethics Committee of Shanxi Medical University (No. SYDL2021004).

ORCID

Jimin Cao https://orcid.org/0000-0002-6546-555X

REFERENCES

1. Mackall JA, Carlson MD. Ventricular and supraventricular arrhythmias in acute myocardial infarction. In: Allen J, Brown DL, eds. *Cardiac Intensive Care*. 2nd ed. Saunders; 2010:241-250.
2. Jardine DL, Charles CJ, Forrester MD, Whitehead M, Nicholls MG. A neural mechanism for sudden death after myocardial infarction. *Clin Auton Res*. 2003;13(5):339-341. doi:10.1007/s10286-003-0109-3
3. Zhai XW, Zhang L, Guo YF, et al. The I_{K1}/Kir2.1 channel agonist zacopride prevents and cures acute ischemic arrhythmias in the rat. *PLoS One*. 2017;12(5):e0177600. doi:10.1371/journal.pone.0177600
4. Janse MJ. Electrophysiological changes in heart failure and their relationship to arrhythmogenesis. *Cardiovasc Res*. 2004;61(2):208-217. doi:10.1016/j.cardiores.2003.11.018
5. Anumonwo JM, Lopatin AN. Cardiac strong inward rectifier potassium channels. *J Mol Cell Cardiol*. 2010;48(1):45-54. doi:10.1016/j.yjmcc.2009.08.013
6. Lopatin AN, Anumonwo JM. Structural and molecular bases of cardiac inward rectifier Potassium Channel function. In: Zipes DP, Jalife J, Stevenson WG, eds. *Cardiac Electrophysiology: From Cell to Bedside*. 7th ed. WB Saunders Co.; 2014:38-48.
7. Molkentin JD, Lu JR, Antos CL, et al. A calcineurin-dependent transcriptional pathway for cardiac hypertrophy. *Cell*. 1998;93(2):215-228. doi:10.1016/s0092-8674(00)81573-1
8. Zhang T, Brown JH. Role of Ca^{2+}/calmodulin-dependent protein kinase II in cardiac hypertrophy and heart failure. *Cardiovasc Res*. 2004;63(3):476-486. doi:10.1016/j.cardiores.2004.04.026
9. Fox DJ, Klein GJ, Hahn A, et al. Reduction of complex ventricular ectopy and improvement in exercise capacity with flecainide therapy in Andersen-Tawil syndrome. *Europace*. 2008;10(8):1006-1008. doi:10.1093/europace/eun180
10. Miyamoto K, Aiba T, Kimura H, et al. Efficacy and safety of flecainide for ventricular arrhythmias in patients with Andersen-Tawil syndrome with KCNJ2 mutations. *Heart Rhythm*. 2015;12(3):596-603. doi:10.1016/j.hrthm.2014.12.009
11. Caballero R, Dolz-Gaitón P, Gómez R, et al. Flecainide increases Kir2.1 currents by interacting with cysteine 311, decreasing the polyamine-induced rectification. *Proc Natl Acad Sci U S A*. 2010;107(35):15631-15636. doi:10.1073/pnas.1004021107
12. Zhai X, Qiao X, Zhang L, et al. I_{K1} channel agonist zacopride suppresses ventricular arrhythmias in conscious rats with healing myocardial infarction. *Life Sci*. 2019;239:117075. doi:10.1016/j.lfs.2019.117075
13. Liu C, Liu E, Luo T, Zhang W, He R. Opening of the inward rectifier potassium channel alleviates maladaptive tissue repair following myocardial infarction. *Acta Biochim Biophys Sin*. 2016;48(8):687-695. doi:10.1093/abbs/gmw060
14. Liu QH, Qiao X, Zhang LJ, et al. I_{K1} channel agonist zacopride alleviates cardiac hypertrophy and failure *via* alterations in calcium dyshomeostasis and electrical remodeling in rats. *Front Pharmacol*. 2019;10:929. doi:10.3389/fphar.2019.00929
15. Liu QH, Zhang LJ, Wang J, Wu BW, Cao JM. Cardioprotection of an I_{K1} channel agonist on L-thyroxine induced rat ventricular remodeling. *Am J Transl Res*. 2021;13(8):8683-8696.
16. Pushpakom S, Iorio F, Eyers PA, et al. Drug repurposing: progress, challenges and recommendations. *Nat Rev Drug Discov*. 2019;18(1):41-58. doi:10.1038/nrd.2018.168
17. Talevi A, Bellera CL. Challenges and opportunities with drug repurposing: finding strategies to find alternative uses of therapeutics. *Expert Opin Drug Discov*. 2020;15(4):397-401. doi:10.1080/17460441.2020.1704729
18. Ashburn TT, Thor KB. Drug repositioning: identifying and developing new uses for existing drugs. *Nat Rev Drug Discov*. 2004;3(8):673-683. doi:10.1038/nrd1468
19. Reynolds JEF. *Martindale: The Extra Pharmacopoeia*. 31st ed. Royal Pharmaceutical Society; 1996.
20. Huang SS, Tsai SK, Chiang LY, Tsai LM. Cardioprotective effects of hexasulfobutylated C60 (FC4S) in anesthetized rats during coronary occlusion/reperfusion injury. *Drug Dev Res*. 2001;53:244-253.
21. Curtis MJ, Hancox JC, Farkas A, et al. The Lambeth conventions (II): guidelines for the study of animal and human ventricular and supraventricular arrhythmias. *Pharmacol Ther*. 2013;139(2):213-248. doi:10.1016/j.pharmthera.2013.04.008
22. Branco AF, Pereira SP, Gonzalez S, Gusev O, Rizvanov AA, Oliveira PJ. Gene expression profiling of H9c2 myoblast differentiation towards a cardiac-like phenotype. *PLoS One*. 2015;10(6):e0129303. doi:10.1371/journal.pone.0129303
23. Li X, Hu H, Wang Y, et al. Valsartan upregulates Kir2.1 in rats suffering from myocardial infarction via casein kinase 2. *Cardiovasc Drugs Ther*. 2015;29(3):209-218. doi:10.1007/s10557-015-6598-1
24. Harding SD, Sharman JL, Faccenda E, et al. The IUPHAR/BPS guide to PHARMACOLOGY in 2018: updates and expansion to encompass the new guide to IMMUNOPHARMACOLOGY. *Nucleic Acids Res*. 2018;46(D1):D1091-D1106. doi:10.1093/nar/gkx1121
25. Alexander SP, Mathie A, Peters JA, et al. THE CONCISE GUIDE TO PHARMACOLOGY 2021/22: ion channels. *Br J Pharmacol*. 2021;178(Suppl 1):S157-S245. doi:10.1111/bph.15539
26. Fauconnier J, Lacampagne A, Rauzier JM, et al. Frequency-dependent and proarrhythmogenic effects of FK-506 in rat ventricular cells. *Am J Physiol Heart Circ Physiol*. 2005;288(2):H778-H786. doi:10.1152/ajpheart.00542.2004
27. Blandin CE, Gravez BJ, Hatem SN, Balse E. Remodeling of Ion Channel trafficking and cardiac arrhythmias. *Cell*. 2021;10(9):2417. doi:10.3390/cells10092417
28. Vaidyanathan R, Taffet SM, Vikstrom KL, Anumonwo JM. Regulation of cardiac inward rectifier potassium current (I[K1]) by synapse-associated protein-97. *J Biol Chem*. 2010;285(36):28000-28009. doi:10.1074/jbc.M110.110858
29. Hibino H, Inanobe A, Furutani K, Murakami S, Findlay I, Kurachi Y. Inwardly rectifying potassium channels: their structure, function, and physiological roles. *Physiol Rev*. 2010;90(1):291-366. doi:10.1152/physrev.00021.2009
30. Lee TM, Lin MS, Chang NC. Effect of ATP-sensitive potassium channel agonists on ventricular remodeling in healed rat infarcts. *J Am Coll Cardiol*. 2008;51(13):1309-1318. doi:10.1016/j.jacc.2007.11.067

31. Sun JM, Wang CM, Guo Z, et al. Reduction of isoproterenol-induced cardiac hypertrophy and modulation of myocardial connexin43 by a KATP channel agonist. *Mol Med Rep*. 2015;11(3):1845-1850. doi:10.3892/mmr.2014.2988
32. Varro A, Nanasi PP, Acsai K, Virag L, Papp JG. Cardiac sarcolemmal ion channels and transporters as possible targets for antiarrhythmic and positive inotropic drugs: strategies of the past-perspectives of the future. *Curr Pharm des*. 2004;10(20):2411-2427. doi:10.2174/1381612043383836
33. Kumar M, Haghighi K, Kranias EG, Sadayappan S. Phosphorylation of cardiac myosin-binding protein-C contributes to calcium homeostasis. *J Biol Chem*. 2020;295(32):11275-11291. doi:10.1074/jbc.RA120.013296
34. McDonald TF, Pelzer S, Trautwein W, Pelzer DJ. Regulation and modulation of calcium channels in cardiac, skeletal, and smooth muscle cells. *Physiol Rev*. 1994;74(2):365-507. doi:10.1152/physrev.1994.74.2.365
35. Roe AT, Frisk M, Louch WE. Targeting cardiomyocyte Ca^{2+} homeostasis in heart failure. *Curr Pharm des*. 2015;21:431-448.
36. Hegyi B, Morotti S, Liu C, et al. Enhanced depolarization drive in failing rabbit ventricular myocytes: calcium-dependent and β-adrenergic effects on late sodium, L-type calcium, and sodium-calcium exchange currents. *Circ Arrhythm Electrophysiol*. 2019;12(3):e007061. doi:10.1161/CIRCEP.118.007061
37. Hegyi B, Bossuyt J, Ginsburg KS, et al. Altered repolarization reserve in failing rabbit ventricular myocytes: calcium and β-adrenergic effects on delayed- and inward-rectifier potassium currents. *Circ Arrhythm Electrophysiol*. 2018;11(2):e005852. doi:10.1161/CIRCEP.117.005852
38. Swynghedauw B. Molecular mechanisms of myocardial remodeling. *Physiol Rev*. 1999;79(1):215-262. doi:10.1152/physrev.1999.79.1.215
39. Matsuda H, Cruz JS. Voltage-dependent block by internal Ca^{2+} ions of inwardly rectifying K^+ channels in Guinea-pig ventricular cells. *J Physiol*. 1993;470:295-311. doi:10.1113/jphysiol.1993.sp019859
40. Zaza A, Rocchetti M, Brioschi A, Cantadori A, Ferroni A. Dynamic Ca^{2+}–induced inward rectification of K^+ current during the ventricular action potential. *Circ Res*. 1998;82(9):947-956. doi:10.1161/01.res.82.9.947
41. Fauconnier J, Lacampagne A, Rauzier JM, Vassort G, Richard S. Ca^{2+}–dependent reduction of I_{K1} in rat ventricular cells: a novel paradigm for arrhythmia in heart failure? *Cardiovasc Res*. 2005;68(2):204-212. doi:10.1016/j.cardiores.2005.05.024
42. Zangerl-Plessl EM, Qile M, Bloothooft M, Stary-Weinzinger A, van der Heyden MAG. Disease associated mutations in K_{IR} proteins linked to aberrant inward rectifier channel trafficking. *Biomolecules*. 2019;9(11):650. doi:10.3390/biom9110650
43. Musa H, Marcou CA, Herron TJ, et al. Abnormal myocardial expression of SAP97 is associated with arrhythmogenic risk. *Am J Physiol Heart Circ Physiol*. 2020;318(6):H1357-H1370. doi:10.1152/ajpheart.00481.2019
44. Leonoudakis D, Conti LR, Radeke CM, McGuire LM, Vandenberg CA. A multiprotein trafficking complex composed of SAP97, CASK, Veli, and Mint1 is associated with inward rectifier Kir2 potassium channels. *J Biol Chem*. 2004;279(18):19051-19063. doi:10.1074/jbc.M400284200
45. Saad NS, Elnakish MT, Ahmed AAE, Janssen PML. Protein kinase a as a promising target for heart failure drug development. *Arch Med Res*. 2018;49(8):530-537. doi:10.1016/j.arcmed.2018.12.008
46. Wang J, Liu X, Arneja AS, Dhalla NS. Alterations in protein kinase a and protein kinase C levels in heart failure due to genetic cardiomyopathy. *Can J Cardiol*. 1999;15(6):683-690.
47. Zhang X, Szeto C, Gao E, et al. Cardiotoxic and cardioprotective features of chronic β-adrenergic signaling. *Circ Res*. 2013;112(3):498-509. doi:10.1161/CIRCRESAHA.112.273896
48. Prabu SK, Anandatheerthavarada HK, Raza H, Srinivasan S, Spear JF, Avadhani NG. Protein kinase A-mediated phosphorylation modulates cytochrome c oxidase function and augments hypoxia and myocardial ischemia-related injury. *J Biol Chem*. 2006;281(4):2061-2070. doi:10.1074/jbc.M507741200
49. Yu QJ, Si R, Zhou N, et al. Insulin inhibits beta-adrenergic action in ischemic/reperfused heart: a novel mechanism of insulin in cardioprotection. *Apoptosis*. 2008;13(2):305-317. doi:10.1007/s10495-007-0169-2
50. Kalscheur MM, Vaidyanathan R, Orland KM, et al. KCNJ2 mutation causes an adrenergic-dependent rectification abnormality with calcium sensitivity and ventricular arrhythmia. *Heart Rhythm*. 2014;11(5):885-894. doi:10.1016/j.hrthm.2014.02.015
51. Wischmeyer E, Karschin A. Receptor stimulation causes slow inhibition of IRK1 inwardly rectifying K^+ channels by direct protein kinase A-mediated phosphorylation. *Proc Natl Acad Sci U S A*. 1996;93(12):5819-5823. doi:10.1073/pnas.93.12.5819
52. Koumi S, Backer CL, Arentzen CE, Sato R. Beta-adrenergic modulation of the inwardly rectifying potassium channel in isolated human ventricular myocytes. Alteration in channel response to beta-adrenergic stimulation in failing human hearts. *J Clin Invest*. 1995;96(6):2870-2881. doi:10.1172/JCI118358
53. Pare GC, Bauman AL, McHenry M, Michel JJ, Dodge-Kafka KL, Kapiloff MS. The mAKAP complex participates in the induction of cardiac myocyte hypertrophy by adrenergic receptor signaling. *J Cell Sci*. 2005;118(Pt 23):5637-5646. doi:10.1242/jcs.02675
54. Valentine CD, Haggie PM. Confinement of β(1)- and β(2)-adrenergic receptors in the plasma membrane of cardiomyocyte-like H9c2 cells is mediated by selective interactions with PDZ domain and A-kinase anchoring proteins but not caveolae. *Mol Biol Cell*. 2011;22(16):2970-2982. doi:10.1091/mbc.E11-01-0034
55. Dart C, Leyland ML. Targeting of an a kinase-anchoring protein, AKAP79, to an inwardly rectifying potassium channel, Kir2.1. *J Biol Chem*. 2001;276(23):20499-20505. doi:10.1074/jbc.M101425200
56. Plaster NM, Tawil R, Tristani-Firouzi M, et al. Mutations in Kir2.1 cause the developmental and episodic electrical phenotypes of Andersen's syndrome. *Cell*. 2001;105(4):511-519. doi:10.1016/s0092-8674(01)00342-7
57. Xia M, Jin Q, Bendahhou S, et al. A Kir2.1 gain-of-function mutation underlies familial atrial fibrillation. *Biochem Biophys Res Commun*. 2005;332(4):1012-1019. doi:10.1016/j.bbrc.2005.05.054
58. Jalife J. Inward rectifier potassium channels control rotor frequency in ventricular fibrillation. *Heart Rhythm*. 2009;6(11 Suppl):S44-S48. doi:10.1016/j.hrthm.2009.07.019
59. Zhang H, Garratt CJ, Zhu J, Holden AV. Role of up-regulation of I_{K1} in action potential shortening associated with atrial fibrillation in humans. *Cardiovasc Res*. 2005;66(3):493-502. doi:10.1016/j.cardiores.2005.01.020
60. Gaborit N, Le Bouter S, Szuts V, et al. Regional and tissue specific transcript signatures of ion channel genes in the non-diseased human heart. *J Physiol*. 2007;582(Pt 2):675-693. doi:10.1113/jphysiol.2006.126714

SUPPORTING INFORMATION

Additional supporting information can be found online in the Supporting Information section at the end of this article.

How to cite this article: Liu Q, Sun J, Dong Y, et al. Tetramisole is a new I_{K1} channel agonist and exerts I_{K1}-dependent cardioprotective effects in rats. *Pharmacol Res Perspect*. 2022;10:e00992. doi:10.1002/prp2.992